

Non differentiable large-deviation functionals in boundary-driven diffusive systems

Guy Bunin, Yariv Kafri, and Daniel Podolsky
 Technion – Israel Institute of Technology, Haifa 32000, Israel

We study the probability of arbitrary density profiles in conserving diffusive fields which are driven by the boundaries. We demonstrate the existence of singularities in the large-deviation functional, the direct analog of the free-energy in non-equilibrium systems. These singularities are unique to non-equilibrium systems and are a direct consequence of the breaking of time-reversal symmetry. This is demonstrated in an exactly-solvable model and also in numerical simulations on a boundary-driven Ising model. We argue that this singular behavior is expected to occur in models where the compressibility has a deep enough minimum. The mechanism is explained using a simple model.

PACS numbers: 05.40.-a, 05.70.Ln, 5.10.Gg, 05.50.+q

Consider a field $\rho(x)$ with diffusive dynamics which are conserving in the bulk. Here, $\rho(x)$ could describe the density of a gas in a capillary connecting two reservoirs. When the reservoirs are of equal density $\bar{\rho}$, the system is in equilibrium. Then the steady-state probability $P[\rho_f]$ of an arbitrary density profile $\rho_f(x)$ is given by $P[\rho_f] \sim e^{-F[\rho_f]/k_B T}$, where F is the free-energy. Generically, for a system with short-range interactions, F is a local functional of $\rho_f(x)$ and, in the disordered phase, it is a smooth functional. For instance, when the particles in the capillary interact only through hard-core exclusion, $F[\rho_f] = N \int_0^1 dx \{ \rho_f(x) \log \frac{\rho_f(x)}{\bar{\rho}} + (1 - \rho_f(x)) \log \frac{1 - \rho_f(x)}{1 - \bar{\rho}} \}$, where N is the length of the capillary and the density is normalized such that $\rho = 1$ corresponds to a filled capillary.

A fundamental goal of non-equilibrium statistical mechanics is to evaluate and understand the general structure of $P[\rho_f]$ when the densities of the two reservoirs are different, such that a current flows through the system. For diffusive systems there has been great progress in recent years, and by now several important properties of $P[\rho_f]$ have been established. For example, it is known that $P[\rho_f] \sim e^{-N^d \phi[\rho_f]}$, where N^d is the volume of the system and $\phi[\rho_f]$ is a non-equilibrium analogue of the free energy, called the large deviation functional (LDF). It attains a minimum at the most probable density profile and, when the system is driven out of equilibrium, it becomes a *non-local functional* of $\rho_f(x)$. This has important consequences, manifested for example through long range correlations which are present even when the interactions are strictly local [1, 2]. In contrast to equilibrium the LDF depends on the dynamics, and not only on the Boltzmann weights.

Recently, framework within which $\phi[\rho_f]$ can be calculated has been laid out, building on standard tools from the theory of large deviations [3–8]. The key observation is that in these systems the probability of an atypical event is dominated by a single history leading up to it, and starting from the most probable profile; other histories are exponentially less likely in the system size. While calculating the LDF within the framework is in general extremely difficult, it has allowed to establish exact solutions in a number of simple models [4, 9] (in some cases building on solutions obtained by other methods [10]).

In addition, the framework has led to efficient numerical algorithms for evaluating $P[\rho_f]$ for arbitrary diffusive models [11], as well as LDFs of global quantities such as the current [12–15].

Despite the successes, a general understanding of the properties of $P[\rho_f]$ out of equilibrium is lacking. For example, for boundary-driven currents induced by reservoirs held at different densities, $\phi[\rho_f]$ is a smooth functional of ρ_f for particles diffusing with hard-core exclusion, just as in equilibrium [10]. In stark contrast, in the presence of a strong bulk drive (for example, when a constant force acts on the particles in the capillary) $\phi[\rho_f]$ becomes non-analytic [16]. This is due to the existence of multiple histories leading to the same ρ_f with comparable weight, and immediately implies singular behavior in the LDF of other more global quantities. These singularities are more subtle than those observed for the current or particle number [17–20], which can arise even if the LDF on the phase space is smooth, hence even in equilibrium models (in contrast to the present phenomenon, see below). It is far from clear which models exhibit such singular behavior, and how to characterize these singularities. It is natural to ask whether these singularities can appear when no bulk drive is present.

In this Letter we study boundary-driven diffusive systems and show for the first time that singular behavior in ϕ can indeed occur in these systems. We first provide an example of an exactly solvable model which exhibits such a singularity. Then we use numerics to demonstrate that this phenomenon occurs in a broad class of models (for example, in a boundary-driven Ising model). We elucidate the mechanism by which the singularities arise, by introducing a simple model which contains the essential ingredients leading to the singularity. This model shows the close connection between the singularities and a spontaneous symmetry breaking. We provide guidelines to systems which can be expected to show this singular behavior. Throughout our analysis we use analogies with previous works on the Fokker-Planck equation in the presence of small noise. Singular behaviors in such models have been studied extensively in the past [21–26], and we draw analogies with these works whenever possible.

Background theory – We study large deviations of bulk-

conserving diffusive systems which are driven out of equilibrium by the boundaries. For simplicity we consider one dimension, with $0 \leq x \leq 1$. The conserved density $\rho(x, t)$ is related to the current $J(x, t)$ by $\partial_t \rho + \partial_x J = 0$, where the current is given by

$$J = -D(\rho(x, t)) \partial_x \rho(x, t) + \sqrt{\sigma(\rho(x, t))} \eta(x, t) . \quad (1)$$

$D(\rho(x, t))$ is a density-dependent diffusivity function, while $\sigma(\rho(x, t))$ controls the amplitude of the white noise $\eta(x, t)$, which satisfies $\langle \eta(x, t) \rangle = 0$ and $\langle \eta(x, t) \eta(x', t') \rangle = N^{-1} \delta(x - x') \delta(t - t')$. The prefactor N^{-1} in the noise variance results from the fact that we have scaled distances by the system size N , and time by N^2 . After this rescaling the noise is small due to the system size, as a consequence of the coarse graining and rescaling. Eq. (1) describes a broad range of transport phenomena, including electronic systems, ionic conductors, and heat conduction [5, 27, 28]. $D(\rho)$ and $\sigma(\rho)$ are related via a fluctuation-dissipation relation, which for particle systems reads $\sigma(\rho) = 2k_B T \rho^2 \kappa(\rho) D(\rho)$ where $\kappa(\rho)$ is the compressibility [2]. For example, for diffusing hard-core particles, $D = 1$ and $\sigma = 2\rho(1 - \rho)$ [2]. The system is attached to reservoirs which fix the densities at the boundaries of the segment, $\rho(0) = \rho_L$ and $\rho(1) = \rho_R$. If $\rho_L \neq \rho_R$ a current is induced through the system, driving it out of equilibrium.

The average, or most probable density profile for the system $\bar{\rho}$, is obtained by solving $\partial_x [D(\bar{\rho}) \partial_x \bar{\rho}] = 0$, with $\bar{\rho}(0) = \rho_L$ and $\bar{\rho}(1) = \rho_R$ at the boundaries. In equilibrium (i.e. when $\rho_L = \rho_R$), the steady-state probability of any other density profile $\rho(x)$ is easy to obtain – the LDF $\phi[\rho]$ is then given by the free-energy which is local in ρ , $\phi[\rho] = \int f(\rho, \bar{\rho}) dx$, where

$$f(\rho, r) \equiv \int_r^\rho d\rho_1 \int_r^{\rho_1} d\rho_2 \frac{2D(\rho_2)}{\sigma(\rho_2)} . \quad (2)$$

Note that in this case $\bar{\rho}$ is constant, $\bar{\rho} = \rho_L = \rho_R$. By contrast, the steady-state probability distribution away from equilibrium is notoriously hard to compute, and *very* different from the naive guess $\phi[\rho] = \int f(\rho, \bar{\rho}) dx$, now with space dependent $\bar{\rho}(x)$. In fact, as stated above, $\phi[\rho]$ is non-local.

To compute the large deviation for the model described above, one uses the fact that the probability of a history $\{\rho(x, t), J(x, t)\}$ during time $-\infty \leq t \leq 0$ is $P \sim \exp(-NS)$, where the action S is given by [3–7]

$$S = \int_{-\infty}^0 dt \int_0^1 dx \frac{[J(x, t) + D(\rho(x, t)) \partial_x \rho(x, t)]^2}{2\sigma(\rho(x, t))} . \quad (3)$$

For large N , the probability $P \sim e^{-N\phi[\rho_f]}$ is given by $\phi[\rho_f] = \inf_{\rho, J} S$, where the infimum is over histories satisfying $\partial_t \rho + \partial_x J = 0$, with initial and final conditions $\rho(x, t \rightarrow -\infty) = \bar{\rho}(x)$, $\rho(x, t = 0) = \rho_f(x)$, and boundary conditions $\rho(x = 0, t) = \rho_L$ and $\rho(x = 1, t) = \rho_R$.

In many cases, including in equilibrium and in previously studied exactly solvable non-equilibrium models

[9, 10], the action S in Eq. (3) has a single local minimum and $\phi[\rho_f]$ is then a smooth functional. However, as we show below this need not be the case. The action can, in general, have more than one local minimum in the space of histories $\{\rho(x, t), J(x, t)\}$. In regions of the space of final states where ρ_f has more than one minimal history leading to it, the global minimum might switch between two locally minimizing solutions. This is analogous to a first-order phase transition in equilibrium statistical mechanics, where the system switches between two metastable states, which are both local minima of the free-energy. The transition between local minima is accompanied by a jump in the functional derivative of the large-deviation $\delta\phi/\delta\rho$. We will therefore refer to it as a Large Deviation Singularity (LDS). This phenomenon, first studied by Graham and Tél [21], is unique to non-equilibrium: in equilibrium ϕ is smooth whenever the dynamical model (Langevin equation) contains only smooth functions. Note that while LDSs are expected to be generic in models where the zero-noise dynamics feature a number of basins, or unstable fixed points, here the only fixed point is $\bar{\rho}(x)$, and therefore the existence of the singularity is not guaranteed, and indeed is not present in the previously studied models [4, 9, 10].

We first study this phenomenon in an exactly solvable model, and then consider its generalizations.

Exactly solvable model – Consider the model in Eq. (1) with $D = 1$ and a quadratic $\sigma(\rho) = 1 + \rho^2$, a parabola clear above the axis [29]. In [9] it was shown that the LDF is given by $\phi[\rho_f] = \min \phi_{ext}$, where ϕ_{ext} are extremal values of the action given by

$$\phi_{ext} = \int_0^1 dx \left\{ f(\rho_f(x), g(x)) - \ln \frac{g'(x)}{\bar{\rho}'(x)} \right\}$$

where $f(\rho, g)$ is defined in Eq. (2) and $g(x)$ is an auxiliary function satisfying the differential equation

$$0 = \frac{g(x) - \rho_f(x)}{\sigma(g(x))} - \frac{g''(x)}{[g'(x)]^2} , \quad (4)$$

with boundary conditions $g(0) = \rho_L$, and $g(1) = \rho_R$. Note that as $D = 1$, the most probable configuration $\bar{\rho}(x)$ is linear, with $\bar{\rho}(0) = \rho_L$ and $\bar{\rho}(1) = \rho_R$. As we now show, solutions to the differential equation Eq. (4) with initial and final boundary conditions may be non-unique, i.e. there exist profiles $\rho_f(x)$ for which more than one solution $g(x)$ exists. Eq. (4) is solved via a numerical shooting method [30]: here we treat the problem as an initial value problem with initial conditions $g(0) = \rho_L$, and $g'(0) = c$, and scan systematically over values of c to find solutions with $g(1) = \rho_R$. This type of exhaustive search ensures that all extremal states are discovered.

To illustrate the existence of multiple solutions, we consider profiles of the form $\rho_f(x) = \bar{\rho}(x) + \alpha_1 \cos(\pi x/2) + \alpha_2 \sin(\pi x)$, varying α_1 and α_2 , and with boundary-conditions $\rho_L = -3, \rho_R = 3$. Fig. 1(a) shows an example of a profile ρ_f for which only one solution $g(x)$ to Eq. (4) exists. In contrast, in Fig. 1(b) a profile

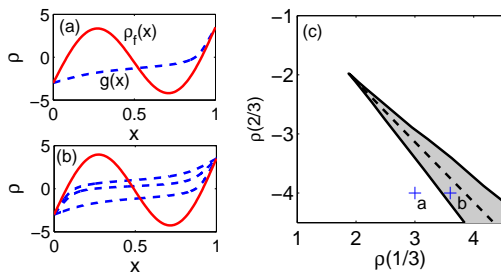


FIG. 1. The model $D = 1, \sigma = \rho^2 + 1$. (a) A profile $\rho_f(x)$ (solid line) with one extremal solution $\phi[\rho]$. The corresponding $g(x)$ also plotted (dashed line). (b) A profile $\rho_f(x)$ with three extremal solutions. (c) Number of extremal solutions as a function of $\rho_f(1/3), \rho_f(2/3)$. Gray region: three solutions. White region: one solution. Also shown are the caustics (solid line), and the switching line (dashed line).

$\rho_f(x)$ with three solutions $g(x)$ is shown, two of them corresponding to local minima, and one to a saddle point. Fig. 1(c) shows the region in which there are multiple solutions. Here we have chosen to parametrize the profiles $\rho_f(x)$ in terms of $\rho_f(1/3)$ and $\rho_f(2/3)$, which are simply related to α_1 and α_2 . Note the marked *caustics*, indicating the boundaries between regions with one and three extremal solutions, and the *switching line*, on which the two locally minimal solutions have the same value for the action. On the switching line the gradient of the LDF is discontinuous [21]; the occurrence of this LDS is the focus of the paper. In addition, the history preceding a rare event is expected to be different on both sides of the switching line, as the history minimizing the action changes. The cusp is found for profiles ρ_f relatively “far” from $\bar{\rho}$, and for $\rho_f(1/3)$ positive and $\rho_f(2/3)$ negative (here $\rho_L < \rho_R$). More generally, the phase space of profiles ρ_f is infinite dimensional, the caustics and switching line become manifolds. The picture shown in Fig. 1(c) is a particular two dimensional cross section. We find similar behavior for ρ_f of similar shapes which are not of the exact form described above.

In fact, for this model one can prove that: (a) for *any* non-equilibrium boundary conditions ($\rho_L \neq \rho_R$) there exist profiles ρ_f for which there is more than one solution to Eq. (4), and (b) profiles which have two locally minimizing histories with the same value of ϕ_{ext} always exist. A proof of these facts will be given elsewhere [31].

The existence of multiple minimizers of S can be intuitively understood as follows: looking at Eq. (3), we see that the contribution to the action is smaller wherever $\sigma(\rho)$ is high. If the variation in $\sigma(\rho)$ is large enough, trajectories passing through regions of high $\sigma(\rho)$ may be favored. If there are two such regions, as around a minimum of σ , there might be different paths of the action utilizing the different favorable $\sigma(\rho)$ regimes. When $D(\rho)$ also varies, we expect the same logic to apply to regions

with high and low $\sigma(\rho)/D(\rho)$. This argument suggests that the phenomenon is robust, and will occur in other modes with similar features, i.e. when $\sigma(\rho)/D(\rho)$ has a pronounced minimum. Below we make this argument precise, but first we demonstrate the generality of the phenomenon by studying it on a different model which admits a concrete microscopic realization.

Boundary driven Ising model – We turn to study a boundary-driven Ising model, a lattice gas with on-site exclusion and nearest-neighbor interaction. (This is a variant of the Katz-Lebowitz-Spohn model [32], but with no bulk bias.) Each site $i = 1, \dots, N$ of a one-dimensional lattice can be either occupied (“1”) or empty (“0”). The jump rate from site i to site $i+1$ depends on the occupation at sites $i-1$ to $i+2$ according to the following rules: $0100 \xrightarrow{1+\delta} 0010, 1101 \xrightarrow{1-\delta} 1011, 1100 \xrightarrow{1+\varepsilon} 1010, 1010 \xrightarrow{1-\varepsilon} 1100$, and their spatially inverted counterparts with identical rates. The parameter $0 < \varepsilon < 1$ corresponds to attractive interactions between the particles; δ controls the density dependence of the mobility. As shown in [33, 34], for each parameter set (ε, δ) one can write implicit analytic equations for $D(\rho)$ which can then be inverted numerically. Then $\sigma(\rho)$ is obtained via the fluctuation-dissipation relation. Fig. 2(a) shows $D(\rho)$ and $\sigma(\rho)$ for $(\varepsilon, \delta) = (0.05, 0.995)$. For equilibrium boundary conditions this model admits an Ising measure.

We now solve for local minimizers of the action S , using the numerical technique described in [11]. The numerical solutions are obtained by gradually changing the end profile ρ_f , while continuously maintaining a locally-minimizing history $\rho(x, t)$. Different locally-minimizing solutions are obtained by changing the final profile to enter the bi-stable region from different directions, see Fig. 2(c). As for the exactly-solvable model, we again find configurations $\rho_f(x)$ for which multiple local minimizers of S exist. In Fig. 2(b), we show two different histories $\rho(x, t)$ leading to the same profile ρ_f , which is chosen again to be of the form: $\rho_f = \bar{\rho}(x) + \alpha_1 \sin \pi x + \alpha_2 \sin 2\pi x$. In Fig. 2(c) we plot the numerically-obtained region in the $\rho_f(1/3), \rho_f(2/3)$ plane with multiple minimizers, together with the “switching line” and the caustics. In addition, for a particular $\rho_f(x)$ we depict the two histories leading to it by showing the time-dependent values of $\rho(x = 2/3, t)$ against $\rho(x = 1/3, t)$. Lines of equal LDF are plotted in Fig. 2(d) to show the jump in its gradient.

Note that in this model and for the chosen parameters, $\sigma(\rho)/D(\rho)$ has a double-hump structure with a deep minimum, so an LDS is expected from the simple considerations discussed above. Indeed, we have experimented with various forms of $D(\rho)$ and $\sigma(\rho)$, and conclude that an LDS occurs when $\sigma(\rho)/D(\rho)$ has a minimum which is deep enough. Recall that by fluctuation-dissipation is related to the compressibility $\sigma(\rho)/D(\rho) = 2k_B T \rho^2 \kappa(\rho)$. These features have to be large enough for this to happen; small changes to a model which does not feature an LDS are generally not enough. When LDSs do appear, we have always found them in regions of phase space

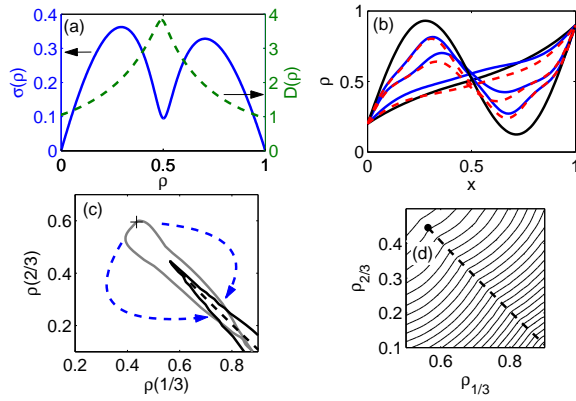


FIG. 2. The boundary-driven Ising model. (a) $D(\rho)$ and $\sigma(\rho)$. (b) Evolution of two locally-minimizing histories leading to the same ρ_f . (c) The coexistence region, showing the caustics (solid black line), switching line (dashed line), and cross-sections of two histories (gray line). Dashed arrows depict paths of the final state in the numerics which yield different local minimizers. (d) Contours of equal LDF (solid lines) and the switching line (dashed).

where the profiles $\rho_f(x)$ have a similar shape to that shown in Fig. 1(b) and Fig. 2(b). The exact conditions and profiles for an LDS to appear must be studied on a model-specific basis. Below we provide a simple model which illustrates the mechanism leading to LDSs in models with these features.

Mechanism – Finally we elucidate the connection between a deep minimum in $\sigma(\rho)$ and the LDS in the configurations discussed above. To do so we introduce a simple sweater sleeve model. We consider a model with $D = 1$ and $\sigma(\rho)$ of order one everywhere except for a narrow range of density values, where it is small:

$$\sigma(\rho) = \begin{cases} \sigma_0 \varepsilon^2 & \rho \in [-\varepsilon/2, \varepsilon/2] \\ \sigma_1(\rho) & \text{otherwise} \end{cases}.$$

Here ε is a small parameter, and $\sigma_1(\rho)$ is some function independent of ε . Then $\sigma(\rho)$ has a deep minimum around $\rho = 0$. (The fact that $\sigma(\rho)$ is discontinuous is not essential – a smoothed version can also be used.)

The key to estimating the action is noting that pushing a mass through the density region $\rho \in [-\varepsilon/2, \varepsilon/2]$ may be costly in terms of the action, creating a “noise barrier”. Consider the cost of passing a small mass element m from $\rho = -\varepsilon/2$ to $\rho = \varepsilon/2$ or vice versa, by applying a current J , see Fig. 3(a). This process is done over a time Δt . The region of space where $\rho \in [-\varepsilon/2, \varepsilon/2]$ is of length Δx . As $J = m/\Delta t$, $\partial_x \rho = \varepsilon/\Delta x$, the action $S = \int dx dt (J + \partial_x \rho)^2 / (2\sigma)$ is, to order $O(\varepsilon^{-1})$,

$$S = \frac{\Delta x \Delta t}{2\sigma_0 \varepsilon^2} \left(\frac{m}{\Delta t} + \frac{\varepsilon}{\Delta x} \right)^2 = \frac{1}{2\sigma_0 \varepsilon^2} \left(m^2 v + \frac{\varepsilon^2}{v} + 2m\varepsilon \right)$$

where $v \equiv \frac{\Delta x}{\Delta t}$. We distinguish between two cases: J “uphill” (against Fick’s law, requiring a strong noise), i.e.

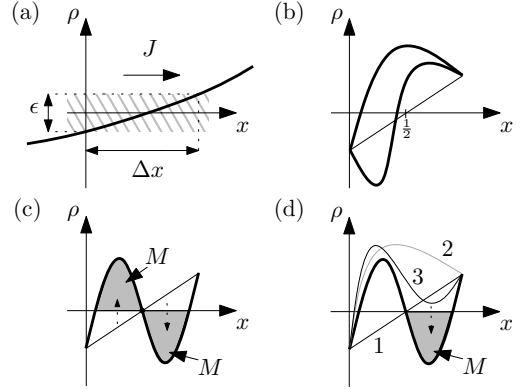


FIG. 3. (a) Passing a mass through the noise barrier $\rho \in [-\varepsilon/2, \varepsilon/2]$. (b) Two profiles which can be reached by only pushing mass “downhill” through the noise barrier. (c) A symmetric history leading to ρ_f requires passing a mass $2M$, shown in gray, “uphill”. (d) A symmetry-breaking history which requires passing only a mass M “uphill”. In (b-d) the straight thin line depicts $\bar{\rho}$, and the bold lines ρ_f .

$\text{sign}(J) = \text{sign}(\partial_x \rho)$, and “downhill” with $\text{sign}(J) = -\text{sign}(\partial_x \rho)$. In the “uphill” case, $\frac{m}{\Delta t}$ and $\frac{\varepsilon}{\Delta x}$ have the same sign, and minimizing S over v we obtain $v = \varepsilon/m$ or $S \geq \frac{2m}{\sigma_0 \varepsilon} + O(\varepsilon^0)$. To push a macroscopic mass M , the bound will then read $S \geq \frac{2M}{\sigma_0 \varepsilon} + O(\varepsilon^0)$. In contrast, if J is “downhill”, $J + \partial_x \rho$ can be made small, with no bound of order $O(\varepsilon^{-1})$.

We now argue that for some profiles ρ_f , such as the one depicted in Fig. 3(c,d), the global minimizing history is not unique. We consider boundary conditions $\rho_L < -\varepsilon/2$ and $\varepsilon/2 < \rho_R$, so that ρ_f crosses the noise barrier three times. To highlight the symmetry-breaking aspect of the phenomenon, we focus on a model with a \mathbb{Z}_2 symmetry where $\sigma_1(\rho) = \sigma_1(-\rho)$, $\rho_L = -\rho_R$, and on a final profile satisfying $\rho_f(x) = -\rho_f(1-x)$. Then $\sigma(\rho)$, D and ρ_f have a symmetry under the combined operation of $\rho \rightarrow -\rho$ and $x \rightarrow 1-x$. Let $\rho^{\text{sym}}(x, t)$ be the minimizer of S subject to this symmetry. In the space of histories it is extremal, but not necessarily the minimizing history. Indeed, we show that other solutions have lower action, spontaneously breaking the symmetry. Referring to Fig. 3(c) we note that in a symmetric history $\rho(x, t)$ we have $\rho(x = 1/2, t) = 0$, and masses in the region shaded in gray, $2M$, must be pushed “uphill” through the $\rho = 0$ line, hence $S \geq \frac{4M}{\sigma_0 \varepsilon}$. However, in the symmetry-breaking history shown in Fig. 3(d) only a mass M has to be pushed “uphill”, so that $S = \frac{2M}{\sigma_0 \varepsilon} + O(\varepsilon^0)$. Therefore, for a small enough ε this solution is favorable. By symmetry, the solution with $\rho \rightarrow -\rho$ and $x \rightarrow 1-x$ has the same action. Therefore the symmetry is spontaneously broken, leading to the LDS with a switching line on profiles obeying this symmetry. Note that some profiles ρ_f , such as those in Fig. 3(b), can be generated by a history which only pushes mass “downhill” through $\rho \in [-\varepsilon/2, \varepsilon/2]$, and the above argument for multiple histories will not

hold. While the above argument emphasizes the breaking of a symmetry, the phenomenon exists even in the absence of an explicit symmetry in either the final configuration or the model, as was demonstrated in the first two models considered.

The non-differentiability shown in Figs. 1(c) and 2(c,d) is perhaps the simplest possible singularity [26].

Due to the high dimensionality of the phase space of profiles, more elaborate structures are possible. Understanding and classifying the possible singularities in these models is an exciting direction for future research.

Acknowledgments - This research was funded by the BSF, ISF, and IRG grants.

[1] H. Spohn, *J. Phys. A: Math. Gen.* 16 (1983)

[2] B. Derrida, *J. Stat. Mech.* P07023 (2007)

[3] L. Bertini, A. De Sole, D. Gabrielli, G. Jona-Lasinio, and C. Landim, *Phys. Rev. Lett.* 87, 040601 (2001)

[4] L. Bertini, A. De Sole, D. Gabrielli, G. Jona-Lasinio, and C. Landim, *J. Stat. Phys.* 107 (2002)

[5] A. N. Jordan, E. V. Sukhorukov, and S. Pilgram, *J. Math. Phys.* 45 4386-4417 (2004)

[6] J. Tailleur, J. Kurchan, and V. Lecomte, *J. Phys. A: Math. Theor.* 41 505001 (2008)

[7] M. I. Freidlin and A. D. Wentzell, *Random Perturbations of Dynamical Systems*, Springer-Verlag (1984)

[8] H. Touchette, R. J. Harris, Large deviation approach to nonequilibrium systems, in R. Klages, W. Just, C. Jarzynski (eds), *Nonequilibrium Statistical Physics of Small Systems: Fluctuation Relations and Beyond*, Wiley-VCH, Weinheim (2012)

[9] L. Bertini, D. Gabrielli, and J. Lebowitz, *J. Stat. Phys.* 121 843 (2005)

[10] B. Derrida, J. L. Lebowitz, and E. R. Speer, *J. Stat. Phys.* 107 (2002)

[11] G. Bunin, Y. Kafri, and D. Podolsky, *EPL* 99 (2012) 20002

[12] C. Giardinà, J. Kurchan, and L. Peliti, *Phys. Rev. Lett.* 96, 120603 (2006)

[13] V. Lecomte and J. Tailleur, *J. Stat. Mech.* P03004 (2007)

[14] J. Tailleur and V. Lecomte, *AIP Conf. Proc.* 1091, 212-219 (2008)

[15] C. Giardinà, J. Kurchan, V. Lecomte and J. Tailleur, *J. Stat. Mech.* 45 4 (2011)

[16] L. Bertini, A. De Sole, D. Gabrielli, G. Jona-Lasinio, and C. Landim, *J. Stat. Mech.* (2010) L11001

[17] L. Bertini, A. De Sole, D. Gabrielli, G. Jona-Lasinio, and C. Landim, *Phys. Rev. Lett.* 94, 030601 (2005)

[18] T. Bodineau and B. Derrida, *Phys. Rev. E* 72, 066110 (2005)

[19] N. Merhav and Y. Kafri, *J. Stat. Mech.* P02011 (2010)

[20] P. I. Hurtado and P. L. Garrido *Phys. Rev. Lett.* 107, 180601 (2011)

[21] R. Graham and T. Tél, *Phys. Rev. Lett.* 52, 9-12 (1984), R. Graham and T. Tél, *J. Stat. Phys.*, Vol. 35, Nos. 5/6 (1984), R. Graham and T. Tél, *Phys. Rev. A* Vol. 33, No. 2 (1986), R. Graham and T. Tél, *Phys. Rev. A* Vol. 31, No. 2 (1985)

[22] F. Moss and P. V. E. McClintock, ed., *Noise in Nonlinear Dynamical Systems*, Cambridge University Press, Cambridge (1989)

[23] D. G. Luchinsky, P. V. E. McClintock, and M. I. Dykman, *Rep. Prog. Phys.*, 61(8):889-997 (1998)

[24] R. S. Maier and D. L. Stein, *Phys. Rev. E*, 48(2):931-938 (1993)

[25] M.I. Dykman, M.M. Millonas and V.N. Smelyanskiy, *Phys. Lett. A*, 195 (1994), 53

[26] M. I. Dykman, D. G. Luchinsky, P. V. E. McClintock, V. N. Smelyanskiy, *Phys. Rev. Lett.* 77 26 (1996)

[27] W. Dieterich, P. Fulde and I. Peschel, *Adv. in Phys.* 29 (1980)

[28] C. Kipnis, C. Marchioro and E. Presutti, *J. Stat. Phys.* 27 65 (1982)

[29] It is easy to show that the phenomenon exists in all models with $D = 1$ and $\sigma(\rho) = a + b\rho^2$ with a, b positive.

[30] W. H. Press, S. A. Teukolsky, W. T. Vetterling and B. P. Flannery, *Numerical Recipes. The Art of Scientific Computing*, 3rd Ed. (2007)

[31] G. Bunin, Y. Kafri and D. Podolsky, in preparation.

[32] S. Katz, J. L. Lebowitz, and H. Spohn, *J. Stat. Phys.*, 34, 3/4 (1984)

[33] H. Spohn, *Large Scale Dynamics of Interacting Particles*, Springer Verlag (1991)

[34] J. S. Hager, J. Krug, V. Popkov and G. M. Schütz, *Phys. Rev. E*, 63, 056110 (2001)